

ErbB2 is essential in the prevention of dilated cardiomyopathy

STEVEN A. CRONE^{1,2,3}, YOU-YANG ZHAO^{2,4}, LIAN FAN⁵, YUSU GU^{2,4}, SUSUMU MINAMISAWA^{2,4}, YANG LIU^{2,4}, KIRK L. PETERSON^{2,4}, JU CHEN^{2,4}, RONALD KAHN⁶, GIANLUIGI CONDORELLI⁷, JOHN ROSS JR^{2,4}, KENNETH R. CHIEN^{2,4} & KUO-FEN LEE^{1,2}

¹The Salk Institute, La Jolla, California, USA

²UCSD-Salk Program in Molecular Medicine, ³Division of Biology,

⁴The Institute of Molecular Medicine, University of California at San Diego, La Jolla, California, USA

⁵Department of Immunology, The Scripps Research Institute, La Jolla, California, USA

⁶Research Division, Joslin Diabetes Center and Department of Medicine, Harvard Medical School, Boston, Massachusetts, USA

⁷Kimmel Cancer Center, Thomas Jefferson University, Philadelphia, Pennsylvania, USA

S.A.C. and Y.-Y.Z. contributed equally to this study.

Correspondence should be addressed to K.F.L.; email: klee@salk.edu

Amplification of the gene encoding the ErbB2 (Her2/neu) receptor tyrosine kinase is critical for the progression of several forms of breast cancer. In a large-scale clinical trial, treatment with Herceptin (trastuzumab), a humanized blocking antibody against ErbB2, led to marked improvement in survival. However, cardiomyopathy was uncovered as a mitigating side effect, thereby suggesting an important role for ErbB2 signaling as a modifier of human heart failure. To investigate the physiological role of ErbB2 signaling in the adult heart, we generated mice with a ventricular-restricted deletion of *ErbB2*. These ErbB2-deficient conditional mutant mice were viable and displayed no overt phenotype. However, physiological analysis revealed the onset of multiple independent parameters of dilated cardiomyopathy, including chamber dilation, wall thinning and decreased contractility. Additionally, cardiomyocytes isolated from these conditional mutants were more susceptible to anthracycline toxicity. ErbB2 signaling in cardiomyocytes is therefore essential for the prevention of dilated cardiomyopathy.

Amplification of the gene encoding the ErbB2 (Her2/neu) receptor tyrosine kinase, a coreceptor for neuregulins^{1,2}, is critical for the progression of several forms of human breast cancer³. Herceptin (trastuzumab), a humanized monoclonal antibody specific for the extracellular domain of ErbB2, has been approved by the United States Food and Drug Administration to treat breast cancers involving overexpression of *ErbB2*. In clinical trials, Herceptin is effective as a single agent, but can also have additive or synergistic effects when used in conjunction with chemotherapeutic agents^{4,5}. However, 7% of patients receiving Herceptin as a second-line therapy, following anthracycline treatment as a first-line therapy, develop cardiac dysfunction. When Herceptin is combined with concurrent treatment with anthracyclines, the incidence of cardiac dysfunction increases to 28% (refs. 4–6). As the vast majority of patients had at one time received anthracycline treatment, the incidence of cardiomyopathy in Herceptin-treated patients in the absence of prior anthracycline treatment has not been determined. Determining the basis of Herceptin-related cardiomyopathy has important implications for designing appropriate therapeutic regimens involving Herceptin as a single agent or adjuvant, as well as devising strategies for preventing or mitigating cardiac dysfunction and heart failure in patients receiving Herceptin. The mechanisms underlying the onset of cardiomyopathy in Herceptin-treated patients could include any of the following:

immune-mediated destruction of cardiomyocytes, drug–drug interaction with anthracyclines, defects in ErbB2 signaling required for maintenance of cardiac contractility, interference with cardiomyocyte survival signals or indirect consequences of Herceptin-mediated effects outside the heart.

Herceptin specifically recognizes the human ErbB2 receptor and does not crossreact with the receptor in other species. Thus, studies of Herceptin-induced cardiotoxicity in animal models would not be informative. To study the role of ErbB2 in adult cardiac function, we have used the Cre-*loxP* system to generate mice containing heart-restricted inactivation of *ErbB2*. These ErbB2-deficient conditional mutant mice were viable and displayed no overt phenotype. However, physiological analysis revealed a progressive onset of multiple independent parameters of dilated cardiomyopathy, the same type of cardiac dysfunction evident in patients treated with Herceptin. In addition, we found that *ErbB2*-deficient cardiomyocytes were more susceptible to anthracycline-induced cell death.

Generation of a cardiac-restricted deletion of ErbB2

We used the Cre-*loxP* system to generate *ErbB2* conditional mutant mice by introducing two *loxP* sites into the *ErbB2* locus to flank a 3-kilobase (kb) region containing the first exon and 1.5 kb of the *ErbB2* promoter. Following expression of Cre recombinase, this critical 3-kb region containing all known

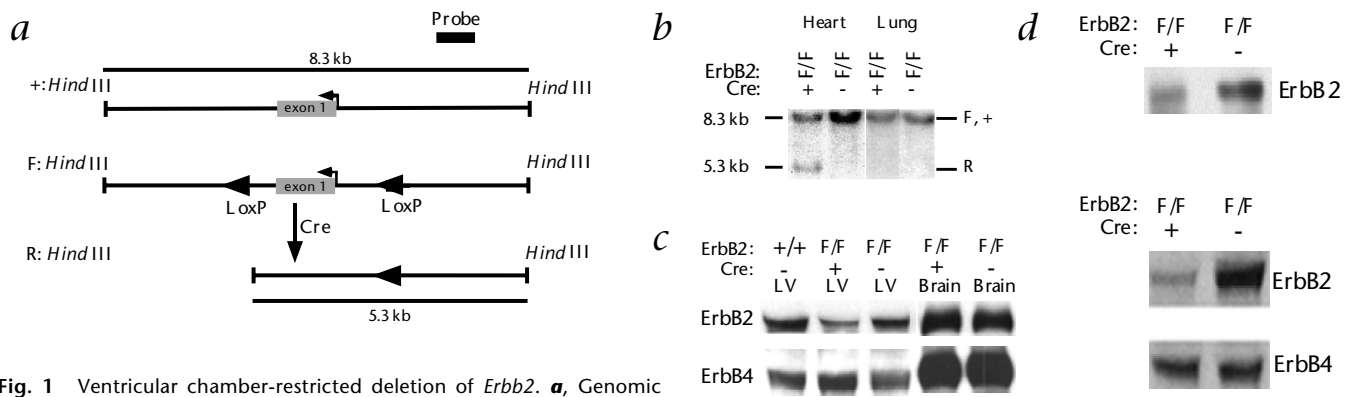


Fig. 1 Ventricular chamber-restricted deletion of *ErbB2*. **a**, Genomic structure of the *ErbB2* wild-type (+), floxed (F), and recombined (R) alleles. Gray box, the first exon; arrow, location and direction of transcription initiation sites; filled triangles, *loxP* sites. **b**, Southern blot demonstrating recombination of the *ErbB2*-floxed allele in the heart, but not lung, of *ErbB2*-floxed/MCK-Cre mice. **c**, Decreased expression of ErbB2, but not ErbB4, protein in *erbB2*-floxed/MLC2v-Cre mice as determined by western-blot analysis of heart extracts. Similar expression of

transcription and translation-initiation sites is excised and *ErbB2* expression is eliminated from the *loxP*-flanked ('floxed') allele (Fig. 1a). To cause recombination of the floxed allele exclusively in cardiac muscle cell lineages, these mice were bred to mice carrying the Cre coding sequence inserted into the endogenous myosin light chain 2v (MLC2v) locus, which can drive high-efficiency ventricular-restricted gene ablations⁷. We used a parallel strategy for ablation of ErbB2 expression based on a well-characterized muscle creatine kinase (MCK)-Cre transgenic mouse that was previously shown to drive high-efficiency recombination in both atrial and ventricular lineages, as well as postnatal skeletal muscle⁸. The resulting mice are called *ErbB2*-floxed/MLC2v-Cre and *ErbB2*-floxed/MCK-Cre mice, respectively, and are collectively referred to as *ErbB2* conditional-knockout (*ErbB2*-CKO) mice.

Both lines of mice exhibit a similar phenotype but differ in the time of onset of cardiomyopathy. As shown by Southern-blot analysis, 32.3 ± 2.5% (*n* = 8) of *ErbB2*-floxed alleles underwent recombination in the ventricular myocardium of *ErbB2*-CKO mice, whereas no evidence of recombination of the floxed allele was found in tissues such as the lung, which do not express Cre (Fig. 1b). Western-blot analysis demonstrated a reduction of ErbB2 protein in the ventricular chamber of *ErbB2*-CKO mice (52 ± 5.4% of controls; *n* = 5; *P* < 0.001), but not a significant change in ErbB4 protein expression (114 ± 4.9% of controls; *n* = 5; *P* = 0.346) (Fig. 1c). Consistent with the elimination of all *ErbB2* expression by the

recombined allele, truncated ErbB2 protein products were not detected in conditional mutants (data not shown). Because only approximately 35% of the cells in an adult heart are cardiomyocytes⁹, the efficiency of recombination in cardiomyocytes should be higher than recombination in the whole tissue. Cardiomyocytes isolated from adult *ErbB2*-CKO mice contained only 29 ± 4.0% of the ErbB2 protein (*n* = 5; *P* < 0.001) of control mice (Fig. 1d), but did not show a significant difference in ErbB4 protein expression (110 ± 4.5%; *n* = 5; *P* = 0.099). Loss of ErbB2 expression occurs perinatally in *ErbB2*-CKO mice. Although no loss of ErbB2 protein expression is detected in the hearts of *ErbB2*-CKO mice at embryonic day 18 (data not shown), cardiomyocytes isolated from neonatal *ErbB2*-CKO mice showed a 40% decrease in ErbB2 protein (Fig. 1d). Consistent with this observation, the numbers of ErbB2-immunoreactive cardiomyocytes are decreased by 44% in cultures derived from *ErbB2*-CKO mice (data not shown). Mice containing at least one wild-type copy of ErbB2 and Cre as well as mice containing two copies of the floxed ErbB2 allele and no Cre were indistinguishable from wild-type mice in all experiments. The efficiency of recombination in *ErbB2*-CKO mice was comparable with previously published reports using the same MCK-Cre or MLC2v-Cre lines to induce recombination of other genes in the heart^{8,10}.

***ErbB2*-CKO mice display features of dilated cardiomyopathy**
The *ErbB2*-CKO mice were recovered at Mendelian frequency,

Table 1 Echocardiographic analysis of *in vivo* cardiac size and function in *ErbB2*-CKO mice

	LVEDD (mm)	LVESD (mm)	FS (%)	SEpth (mm)	PWth (mm)	Mean Vcf (circ/s)	Heart rate (beats/min)	BW (g)	Age (d)
<i>ErbB2</i> -WT (<i>n</i> = 6)	3.73 ± 0.12	2.33 ± 0.10	37.9 ± 2.65	1.05 ± 0.03	1.09 ± 0.04	6.64 ± 0.70	378 ± 29	30.1 ± 2.86	90 ± 1
<i>ErbB2</i> -CKO (<i>n</i> = 8)	4.60 ± 0.20	3.72 ± 0.22	19.4 ± 1.630	94 ± 0.01	0.95 ± 0.03	3.95 ± 0.03	378 ± 19	28.2 ± 1.20	90 ± 1
<i>P</i> value	0.006	0.0005	< 0.0001	0.005	0.01	0.006	1	0.5	1

FS, percent fractional shortening calculated as ((LVEDD - LVESD) / LVEDD) × 100; SEpth, septal wall thickness; PWth, posterior wall thickness; mean Vcf, mean velocity of circumferential fiber shortening; BW, body weight. All values ± s.e.m.

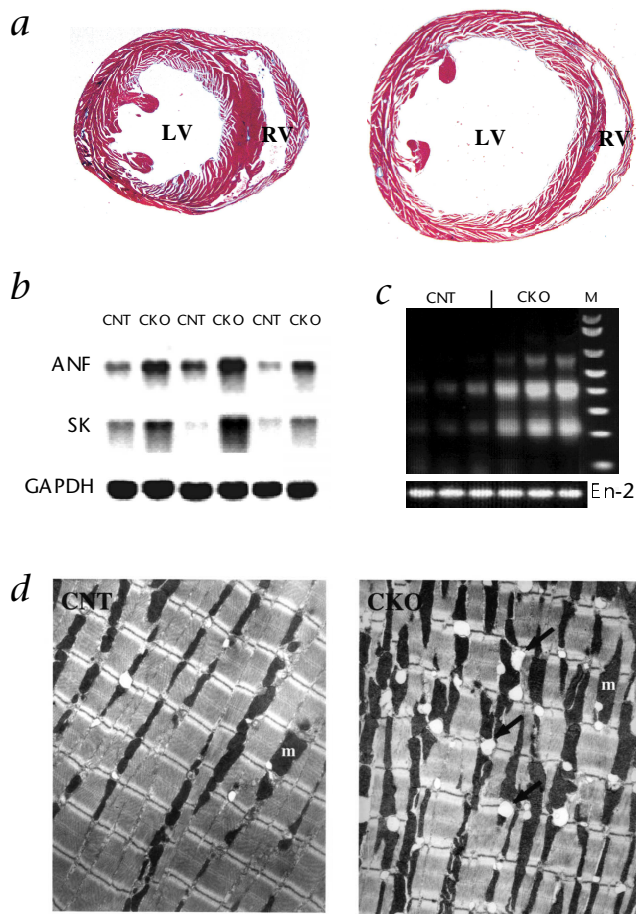


Fig. 2 Phenotypic analyses of *Erbb2*-CKO mice. **a**, Histological analysis of transverse sections stained using trichrome-staining. *Erbb2*-CKO hearts (right) show marked chamber dilation and wall thinning compared with *Erbb2*-floxed hearts (left). **b**, Reactivation of an embryonic gene program in the adult hearts of the *Erbb2*-CKO mice. Northern-blot analysis of *Erbb2* floxed (CNT) and *Erbb2*-Cre (CKO) hearts shows increased expression of mRNA for rat atrial natriuretic factor (ANF) and skeletal α -actin (SK) cDNA probes. GAPDH mRNA was measured to control for gel loading. **c**, Increased apoptosis in the myocardium of *Erbb2*-CKO mice. Following PCR amplification, a DNA ladder indicative of apoptosis is detectable in the genomic DNA from the ventricle of *Erbb2*-CKO mice. M, low-molecular-weight fragments of the 1-kb fragment plus DNA ladder. Amplification of the engrailed-2 (*En-2*) gene was performed as an internal control. **d**, Transmission electron microscopic analysis of sections of LVs reveals increased mitochondria (m) in *Erbb2*-CKO (right) compared with control (left) mice and an increased number of vacuoles (arrows). The contractile apparatus appears intact.

of cardiac hypertrophy, were significantly increased in *Erbb2*-CKO mice compared with controls (Fig. 2b).

Transmission electron microscopy revealed that the numbers of mitochondria and vacuoles in cardiomyocytes from the *Erbb2*-CKO ventricular myocardium was markedly increased, whereas the cytoskeletal ultrastructure were unchanged (Fig. 2d). Notably, increased mitochondria and vacuolization are also observed in human patients suffering from anthracycline cardiotoxicity^{12–14}. Examination of cardiac mitochondrial respiratory function¹⁵ did not reveal any significant differences between *Erbb2*-CKO mice and controls (data not shown). Consistent with an absence of detectable ultrastructural defects, no differences were detected in expression of several cytoskeletal proteins that have been implicated in cardiomyopathy^{16–18}, including utrophin, β -dystroglycan, sarcospan, and α - and γ -sarcoglycan (data not shown).

In vivo cardiac function of *Erbb2*-CKO mice was assessed by several physiological methods, including echocardiography and cardiac catheterization¹⁹. Echocardiography revealed a significant increase in left ventricle (LV) end-diastolic and end-systolic dimensions (LVEDD and LVESD), decreased septal- and posterior-wall thickness, decreased fractional shortening and decreased velocity of circumferential fiber shortening in adult *Erbb2*-CKO mice compared with controls (Table 1). These parameters describe an enlarged LV chamber with thin walls and decreased contractility in *Erbb2*-CKO mice. Retrograde catheterization of the LV via the carotid artery in anesthetized, closed-chest mice revealed a marked reduction of the maximum first derivative of LV pressure (LV dP/dt_{max}) in

display normal cardiac morphogenesis at birth and survive to adulthood. However, histological examination of the hearts from adult *Erbb2*-CKO mice demonstrated ventricular enlargement of both the left and right cardiac chambers, consistent with dilated cardiomyopathy (Fig. 2a). *Erbb2*-CKO mice also showed a marked increase in heart:body-weight ratio (6.32 ± 1.87 mg/g; $n = 8$) versus age- and gender-matched control mice (4.51 ± 0.77 mg/g; $n = 8$; $P < 0.05$). Reactivation of an embryonic gene program is a common feature of many forms of cardiac hypertrophy, including dilated cardiomyopathy¹¹. The mRNA levels of both the atrial natriuretic factor and skeletal α -actin genes, two embryonic genes used as molecular markers

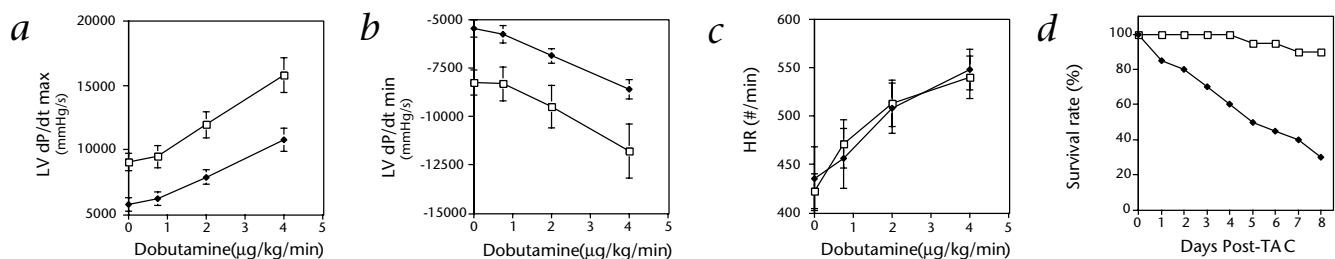


Fig. 3 *Erbb2*-CKO mice display normal responses to dobutamine treatment and decreased survival following pressure overload. Retrograde cardiac catheterization of the LV via the carotid artery was performed under basal conditions and following graded doses of dobutamine in intact anesthetized mice. \square , wild type, $n = 7$; \blacklozenge , *Erbb2*-CKO, $n = 8$. **a**, LV dP/dt_{max} , maximal first derivative of LV pressure. **b**, LV dP/dt_{min} , minimal first derivative of

LV pressure. **c**, HR, heart rate. Data is expressed as mean \pm s.e.m. $P < 0.05$ for controls versus *Erbb2*-CKO mice for LV dP/dt_{max} and LV dP/dt_{min} at all doses of dobutamine. **d**, Survival of control (\blacklozenge) and *Erbb2*-CKO (\square) mice following transverse aortic constriction ($n = 20$). None of the control mice with sham-operation ($n = 3$) or *Erbb2*-CKO mice with sham-operation ($n = 3$) died by day 8.

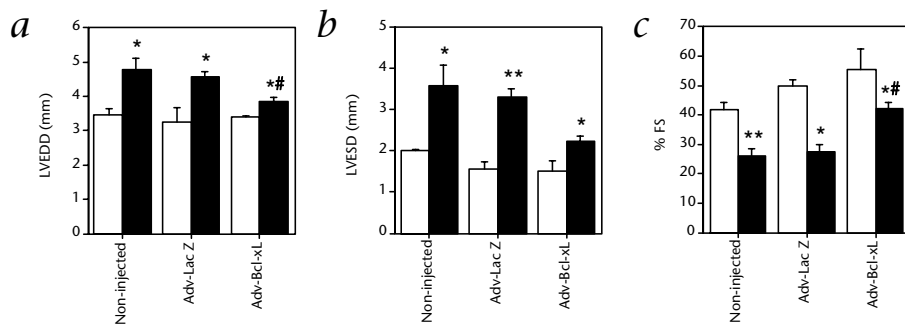


Fig. 4 Prevention of dilated cardiomyopathy in *Erbb2*-CKO mice by overexpression of Bcl-xL. **a–c**, Echocardiography demonstrates that *Erbb2*-CKO mice ($n = 4$, ■) display enlarged LVs (**a** and **b**, non-injected) and decreased contractility (**c**, non-injected) compared with control mice ($n = 4$, □). Adenoviral-mediated expression of Bcl-xL into *Erbb2*-CKO ($n = 8$) partially rescues the enlarged ventricles and decreased contractility observed in non-injected *Erbb2*-CKO mice (**a** and **c**, Adv-Bcl-xL). Injection of a control virus expressing β -gal into *Erbb2*-CKO mice ($n = 3$) does not have a significant effect on chamber dilation or contractility (**a–c**, Adv-LacZ). Bcl-xL expression does not have a significant effect on chamber dilation or contractility in control mice ($n = 3$) (**a–c**). *, $P < 0.05$, CKO versus control mice; **, $P < 0.01$, CKO versus control mice; #, $P < 0.01$ Adv-Bcl-xL CKO, versus non-injected CKO.

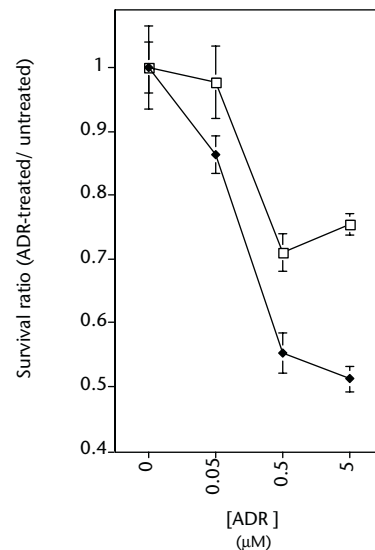
Erbb2-CKO mice (Fig. 3a), demonstrating depressed myocardial contractility consistent with echocardiographic findings. The accompanying reduction in LV dP/dt_{min} (Fig. 3b) indicated that LV relaxation is also markedly impaired. However, there are no significant differences in heart rate, LV end-diastolic pressure (EDP) and tau between the *Erbb2*-CKO and control mice at three months of age (Fig. 3c and data not shown). Isolated single cardiomyocytes from *Erbb2*-CKO mice corroborated the impaired contractility and relaxation demonstrated in the whole heart (data not shown). These data demonstrate that *Erbb2*-CKO mice exhibit several independent, conserved features of human dilated cardiomyopathy.

To determine if *Erbb2*-CKO mice display decreased β -adrenergic responsiveness, a common feature in human heart failure, we assessed the response of LV dP/dt_{max} and LV dP/dt_{min} to graded doses of the β -adrenergic agonist dobutamine. Both contractility (LV dP/dt_{max}) and relaxation (LV dP/dt_{min}) were impaired in *Erbb2*-CKO mice compared with controls at all doses of dobutamine used (Fig. 3a and b). The failure of dobutamine to fully rescue normal cardiac contractility is a pattern seen in clinical cases of moderate, as opposed to severe, heart failure. However, in contrast to some other mouse models of dilated cardiomyopathy^{20,21}, increased doses of dobutamine stimulate increased contractility and relaxation in *Erbb2*-CKO mice, demonstrating that ErbB2 signaling is not required for this physiological response.

Response of *Erbb2*-CKO mice to pressure overload

As ErbB2 and ErbB4 receptors are down-regulated during the transition from hypertrophy to decompensated heart failure²², we investigated the role of ErbB2 signaling in response to the

Fig. 5 Cardiomyocytes from *Erbb2*-CKO mice are more sensitive to adriamycin-induced cell death. Cardiomyocytes were isolated from *Erbb2*-CKO (◆) and control littermates (□) and cultured in concentrations of adriamycin (ADR) ranging from 0.05 to 5.0 μ M. The proportion of surviving cardiomyocytes in ADR-treated cultures versus untreated control cultures is lower in *Erbb2*-CKO cardiomyocytes than control littermates for all concentrations of ADR examined ($n = 3$).



biomechanical stress of pressure overload. Although all of the *Erbb2*-floxed/MCK-Cre mice develop dilated cardiomyopathy by six weeks of age, most *Erbb2*-floxed/MLC2v-Cre mice ($\geq 75\%$) display relatively normal function at this age and progressively acquire features of cardiomyopathy over a six-month time period. Therefore, we performed transthoracic aortic banding²³ on eight-week-old *Erbb2*-floxed/MLC2v-Cre mice prescreened for normal basal cardiac function by echocardiography. The hypertrophic response is preserved in *Erbb2*-floxed/MLC2v-Cre mice following pressure overload, as assessed by heart:body-weight ratio and induction of embryonic gene markers (data not shown). However, *Erbb2*-floxed/MLC2v-Cre mice displayed a significant increase in mortality versus wild-type mice, as shown by a 70% death rate of the

Erbb2-floxed/MLC2v-Cre mice versus 10% in matched wild-type mice (Fig. 3d).

Bcl-xL expression partially rescues dilated cardiomyopathy

Apoptosis is thought to have an important role in dilated cardiomyopathy²⁴. Therefore, we examined whether apoptosis is increased in *Erbb2*-CKO mice. Because very few apoptotic cells are detected in the ventricles of *Erbb2*-CKO by the TUNEL assay (< 4 cells per $1 \times 10^4 \mu\text{m}^2$ of heart section), we used the more sensitive ligation-mediated PCR DNA fragmentation assays to determine whether apoptosis was increased in the myocardium of *Erbb2*-CKO mice. The results show increased apoptosis in the ventricles of *Erbb2*-CKO mice compared with controls (Fig. 2c). The PCR-based assay could not distinguish between apoptosis occurring in cardiomyocytes and other cell types present in the heart.

Although low levels of apoptosis over time could account for the chronic onset of dilated cardiomyopathy occurring in *Erbb2*-CKO mutant mice, these results do not distinguish be-

tween apoptosis as a cause or an effect of cardiomyopathy in these animals. Thus, we determined if over-expression of the anti-apoptotic gene Bcl-xL could rescue the dilated cardiomyopathy in *ErbB2*-CKO mice. Thus, we used a new protocol for high-efficiency, long-term *in vivo* expression in the heart with recombinant adenoviral vectors delivered to the newborn mouse²⁵. For these studies, we used *ErbB2*-floxed/MCK-Cre mice because they display an early onset (by 6 wk of age) of dilated cardiomyopathy. *In vivo* expression of the Bcl-xL gene resulted in the partial rescue of both chamber dilation and contractility in *ErbB2*-floxed/MCK-Cre mutants at six weeks of age (Fig. 4). Both LVEDD and percent fractional shortening (% FS) were significantly reduced in *ErbB2*-floxed/MCK-Cre mice following Bcl-xL expression ($P < 0.01$). The mean LVEDD is reduced in Bcl-xL expressing *ErbB2*-floxed/MCK-Cre mice; however, the results were not statistically significant ($P = 0.08$). Furthermore, following Bcl-xL expression, chamber dilation and contractility of *ErbB2*-floxed/MCK-Cre mice were not significantly different from non-injected control mice ($P > 0.1$ for LVEDD, LVEDD and % FS). Expression of β -galactosidase (β -gal) by an adenovirus control vector in *ErbB2*-floxed/MCK-Cre mice and expression of Bcl-xL in control mice did not demonstrate a statistically significant effect on the same parameters ($P > 0.05$).

The ability of Bcl-xL to prevent, or at least postpone, the onset of dilated cardiomyopathy in *ErbB2*/MCK-Cre mice suggests that apoptosis of cardiomyocytes, or other cell types, contributes to the cardiomyopathy evident in these mice. However, as non-cardiomyocytes may also have a role in the cardiac remodeling that occurs during heart failure²⁶, it is possible that Bcl-xL expression by non-cardiomyocytes is responsible for the rescue of normal heart function. Moreover, it is possible that Bcl-xL mediates important cellular functions in the heart other than prevention of apoptosis in the rescued animals. For example, Bcl-xL may regulate metabolite exchange across outer mitochondrial membranes²⁷ and Ca^{++} signaling²⁸.

Sensitivity to anthracycline in *ErbB2*-CKO cardiomyocytes

Herceptin combined with concurrent treatment with anthracyclines, such as the commonly used anti-cancer agent adriamycin, increases the incidence of cardiac dysfunction in human patients^{4,5}. We examined whether the loss of *ErbB2* leads to increased toxicity of adriamycin in cardiomyocytes isolated from *ErbB2*-CKO mice. Western-blot analysis demonstrated a 40% loss of *ErbB2* protein in neonatal cardiomyocytes isolated from *ErbB2*-floxed/MCK-Cre mice (Fig. 1d), allowing their use in examining effects of *ErbB2* signaling on adriamycin-induced toxicity in culture. Cardiomyocytes isolated from *ErbB2*-CKO mice demonstrated an increased sensitivity to adriamycin toxicity at doses ranging from 0.05 to 5 μ M (Fig. 5). These doses of adriamycin are similar to the serum levels found in patients treated with adriamycin²⁹ as well as the doses used in culture to examine tumor-colony formation²⁹ and cardiotoxicity³⁰. As some cardiomyocytes isolated from neonatal *ErbB2*-CKO mice still express *ErbB2*, the dependence of adriamycin-treated cardiomyocytes on *ErbB2* for survival might be even greater than observed here. Thus, as in the clinical setting, the loss of *ErbB2* signaling in cardiomyocytes aggravates adriamycin-induced toxicity.

Discussion

Here we describe a mouse model in which cardiac-restricted deletion of the *ErbB2* receptor tyrosine kinase leads to dilated

cardiomyopathy. We and others have shown that *ErbB2* has an essential role in the developing embryonic heart^{31–33}. Here we show that *ErbB2* is important in maintaining cardiac function in the adult heart. However, the role of *ErbB2* in the adult heart is distinct from its role during embryogenesis. *ErbB2*-deficient mutants died at embryonic day 10.5 due to improper formation of cardiac trabeculae, the spongy myocardium responsible for maintaining blood flow during early stages of heart morphogenesis. These *ErbB2*-deficient mutants display a morphogenic phenotype, which is unrelated to dilated cardiomyopathy. *ErbB2*-CKO mice show no morphological defects at birth. In fact, most *ErbB2*-floxed/MLC2v-Cre mice displayed normal cardiac structure and function at six weeks of age, and many took up to several months to develop dilated cardiomyopathy. The difference between the onset of cardiomyopathy in *ErbB2*-floxed/MCK-Cre mice versus *ErbB2*-floxed/MLC2v-Cre mice may be due to the fact that MCK-Cre is expressed in atria in addition to ventricles. Alternatively, differences in the genetic background of the two lines of mice may have a role—implicating the existence of modifying loci important for normal heart function in the absence of *ErbB2* signaling.

Previous studies demonstrated that neuregulins promote cardiomyocyte survival *in vitro*³⁴. We demonstrate a small increase in apoptosis in the hearts of *ErbB2*-CKO mice compared with controls and the ability of the anti-apoptotic gene Bcl-xL to partially rescue the dilated cardiomyopathy phenotype. Although our results are consistent with cardiomyocyte apoptosis contributing to the cardiomyopathy observed in *ErbB2*-CKO mice, it is also likely that *ErbB2* is involved in regulating other functions of cardiomyocytes, such as contractility. Further experiments should be conducted to examine other roles of *ErbB2* in mediating normal heart function.

The essential role of *ErbB2* in cardiomyocytes for the prevention of cardiomyopathy suggests that Herceptin-related cardiac dysfunction is not immune-mediated or secondary to effects of Herceptin outside the heart. Furthermore, our findings demonstrate that *ErbB2* does not act solely as a modifier of anthracycline cardiotoxicity, as *ErbB2*-CKO mice display dilated cardiomyopathy in the absence of anthracycline treatment. The interaction between *ErbB2* signaling and anthracycline toxicity is nonetheless clinically important. Using neonatal cardiomyocytes isolated from *ErbB2*-CKO mice, we demonstrate that the loss of *ErbB2* leads to increased sensitivity to anthracycline toxicity. Future experiments aimed at elucidating the molecular basis for this interaction may prove invaluable for preventing cardiomyopathy in patients receiving Herceptin and anthracyclines.

The critical role of *ErbB2* for normal cardiac function suggests that neuregulins or other *ErbB2* agonists may be useful therapeutic agents to prevent Herceptin-related cardiac dysfunction, as well as retard other forms of heart failure. In addition, identifying downstream components of *ErbB2* signaling may lead to new targets for therapeutic agents to treat heart disease. Currently, the use of Herceptin is restricted to treating metastatic breast-cancer patients. However, clinical trials are currently planned or underway to study the effectiveness of Herceptin in treatment of earlier stage breast cancers⁵, and other types of *ErbB2*-overexpressing cancers such as lung, prostate and ovarian cancers³⁵. Thus, preventing Herceptin-mediated cardiomyopathy would not only benefit patients currently approved for Herceptin treatment, but may also

allow broader use of Herceptin to treat other ErbB2-overexpressing cancer patients.

Methods

Generation of mice and histological analyses. A neomycin resistance (neo^r) marker flanked by *loxP* recombination sites was introduced into an *Xba*I site 1.5 kb upstream of the *ErbB2* proximal promoter and first exon (encoding the first 27 amino acids of the N terminus). A third *loxP* site was introduced into a *Bam*HI site (destroyed) in the second intron of *ErbB2* 3-kb downstream of the neo^r marker. The targeting construct contained homologous arms 4.5-kb downstream of the third *loxP* site and 2.8-kb upstream of the first *loxP* site. The targeting construct was electroporated into mouse embryonic stem cells. G418-resistant colonies were isolated and screened by Southern-blot analysis for colonies, which had undergone homologous recombination to include all three *loxP* sites. Positive colonies were then transiently transfected with a plasmid expressing Cre recombinase under control of the CMV promoter. Individual colonies were then screened for those in which the neo^r marker had been removed by Cre-mediated recombination but which still contained the first exon and promoter region of ErbB2 flanked by 2 *loxP* sites (the 'ErbB2-floxed' allele). *ErbB2*-floxed animals were crossed with MLC2v-Cre or MCK-Cre transgenic mice. Hearts from mice at 3–9 months of age were fixed with 4% paraformaldehyde, sectioned and stained by Masson's trichrome method. For electron microscopy, after perfusion fixation with 2% paraformaldehyde-2% glutaraldehyde, tissues from the LV from mice at 3 mo of age were sectioned and stained by the conventional osmium-uranium-lead method. The use of animals is in compliance with the guidelines of the Animal Care and Use Committee of the Salk Institute.

Physiological analyses. Transthoracic echocardiography³⁶, hemodynamic evaluation²⁰ and transverse aortic constriction²³ were performed as described. Avertin (2.5%, 20 μ l/kg body weight), and a xylazine (0.005 mg/g) and ketamine (0.1 mg/g) mixture were used as anesthesia during echocardiography and cardiac catheterization, respectively.

Molecular analyses. Total RNA was isolated from the LV of the *ErbB2*-CKO and control mice. Northern-blot analysis was performed with rat atrial natriuretic factor (ANF) and skeletal α -actin (SK) cDNA probes. The same blots were stripped and rehybridized with a glyceraldehyde 3-phosphate dehydrogenase (GAPDH) cDNA probe to document similar amounts of RNA per lane. Adult ventricular myocytes were isolated by retrograde perfusion with collagenase and separated via two sequential 6% BSA gradients³⁷. Western-blot analysis was performed using Neu (C-18) (Santa Cruz Biotechnology, Santa Cruz, California) and ErbB4 (Neomarkers, Fremont, California) antibodies. In addition, all blots were probed with an actin (C-2) (Santa Cruz Biotechnology, Santa Cruz, California) antibody as a loading control.

Apoptosis assay. A PCR-based DNA fragmentation assay was performed following the protocol provided in the ApoAlert LM-PCR ladder assay kit (Clontech, Palo Alto, California). Mouse En-2 primers were used to amplify the En-2 gene as an internal control. Data shown is representative of 3 independent experiments with nearly identical results.

Adenovirus gene transfer. Adenovirus vectors (containing either β -gal or Bcl-xL coding sequence) were injected into 1-d-old neonatal mouse hearts as described²⁵. 1×10^9 particles/heart were injected into ErbB2/MCK-Cre mice or control littermates. 40 d later, echocardiographic analysis was performed to measure cardiac size and function. Non-injected/*ErbB2*-CKO, $n = 4$; non-injected/control, $n = 4$; Bcl-xL/*ErbB2*-CKO, $n = 8$; Bcl-xL/control, $n = 3$; β -gal/*ErbB2*-CKO, $n = 3$; β -gal/control, $n = 3$.

Cardiomyocyte cultures. Tail DNA of postnatal day 0-1 ErbB2/MCK-Cre or control littermate pups was isolated and used for genotyping. All hearts dissected from mice of the same genotype were pooled, cut into 3 or 4 pieces, and digested in Hank's Balanced Salt Solution (HBSS) plus collagenase (type II, 95 units/ml; Worthington Biochemical, Lakewood,

New Jersey) and pancreatin (1 mg/ml; Sigma) at 37 °C for 10 min. The first digest was discarded and fresh digest solution was added. The hearts were then digested 5 times for 10 min each and the digest solutions added to a half volume of FBS on ice. Inactivated digests were pooled, resuspended in medium containing a 4:1 mix of DMEM and M-199 media plus 10% horse serum and 5% FBS and pre-plated in uncoated flasks twice for 75 min each to remove fibroblasts. The remaining cardiomyocytes were cultured in slide chambers coated with 0.2% gelatin and 12.5 μ g/ml fibronectin at a density of 4,000 cells per cm^2 . After 24 h in culture, media was changed to DMEM/M-199 without serum. 24 h later, the medium was replaced with DMEM/M-199 containing 0–5 μ M adriamycin and 5 ng/ml neuregulin and cultured for an additional 24 h. Cells were then fixed for 10 min in 10% neutral buffered formalin and immunostained with an antibody against sarcomeric α -actinin (Sigma) and anti-mouse Cy-3 secondary antibody (Jackson ImmunoResearch, West Grove, Pennsylvania) and counterstained with DAPI. The number of α -actinin positive cardiomyocytes was counted in 16 random 400- μm^2 microscopic fields for each well. Cultures contained less than 5% fibroblasts. The results, expressed as mean \pm s.e.m., are the average of at least 3 wells for each treatment.

Acknowledgments

We thank K. Campbell and Y. Kobayashi for antibodies against cytoskeletal proteins; R. Gottlieb and R. Sayen for analysis of the function of mitochondria; J. Adams for adenoviral Bcl-xL; Ma. Hoshijima for help with adenovirus injection; and N. Dalton for expertise in echocardiography. The work was supported by NIH grants and The Jean Le Ducq Foundation (to K.R.C. and K.F.L.) and support from an AHA endowed chair and Genentech, Inc (to K.R.C.). S.A.C. is a Markey Predoctoral Fellow and recipient of an award from the Chapman Foundation. K.F.L. is a Pew Scholar.

Competing interests statement

The authors declare competing financial interests: see the website (<http://medicine.nature.com>) for details.

RECEIVED 27 NOVEMBER 2001; ACCEPTED 6 MARCH 2002

- Olayioye, M.A., Neve, R.M., Lane, H.A. & Hynes, N.E. The Erb signaling network: receptor heterodimerization in development and cancer. *EMBO J* **19**, 3159–3167 (2000).
- Klapper, L., Kirschbaum, M.H., Sela, M. & Yarden, Y. Biochemical and clinical implication of the ErbB/HER signaling network of growth factor receptors. *Adv. Cancer Res.* **77**, 25–79 (2000).
- Hynes, N.E. & Stern, D.F. The biology of erbB-2/neu/HER-2 and its role in cancer. *Biochem. Biophys. Acta* **1198**, 165–184 (1994).
- Slamon, D. et al. Use of chemotherapy plus a monoclonal antibody against HER2 for metastatic breast cancer that overexpresses HER2. *New Engl. J. Med.* **344**, 783–792 (2001).
- Baselga, J. Current and planned clinical trials with trastuzumab (Herceptin). *Semin. Oncol.* **27**, 27–32 (2000).
- Sparano, J. Cardiac toxicity of trastuzumab (herceptin): implications for the design of adjuvant trials. *Semin. Oncol.* **28**, 20–27 (2001).
- Chen, J., Kubalak, S.W. & Chien, K.R. Ventricular muscle-restricted targeting of the RXR α gene reveals a non-cell-autonomous requirement in cardiac chamber morphogenesis. *Development* **125**, 1943–1949 (1998).
- Wang, J. et al. Dilated cardiomyopathy and atrioventricular conduction blocks induced by heart-specific inactivation of mitochondrial DNA gene expression. *Nature Genet.* **21**, 133–137 (1999).
- Grove, D., Zak, R., Nair, K.G. & Aschenbrenner, V. Biochemical correlates of cardiac hypertrophy. *Circ. Res.* **25**, 473–485 (1969).
- Hirota, H. et al. Loss of a gp130 cardiac muscle cell survival pathway is a critical event in the onset of heart failure during biomechanical stress. *Cell* **97**, 189–198 (1999).
- Hunter, J.J., Grace, A. & Chien, K.R. Molecular and cellular biology of cardiac hypertrophy and failure. in *Molecular Basis of Cardiovascular Disease: A Companion to Braunwald's Heart Disease* (ed. Chien, K.R.) 211–250 (W.B. Saunders, Philadelphia, 1999).
- Benjamin, R.S., Mason, J.W. & Billingham, M.E. Cardiac toxicity of adriamycin-DNA complex and rubidazole: evaluation by electrocardiogram and endomyocardial biopsy. *Cancer Treat. Rep.* **62**, 935–939 (1978).
- Billingham, M.E., Mason, J.W., Bristow, M.R. & Daniels, J.R. Anthracycline cardiomyopathy monitored by morphologic changes. *Cancer Treat. Rep.* **62**, 865–872 (1978).
- Ferrans, V.J. Overview of cardiac pathology in relation to anthracycline cardiotoxicity. *Cancer Treat. Rep.* **62**, 955–961 (1978).

15. Rustin, P. *et al.* Biochemical and molecular investigations in respiratory chain deficiencies. *Clin. Chim. Acta* **228**, 35–51 (1994).
16. Grady, R.M. *et al.* Skeletal and cardiac myopathies in mice lacking utrophin and dystrophin: a model for duchenne muscular dystrophy. *Cell* **90**, 729–738 (1997).
17. Deconinck, A.E. *et al.* Utrophin-dystrophin-deficient mice as a model for Duchenne muscular dystrophy. *Cell* **90**, 717–727 (1997).
18. Coral-Vazquez, R. *et al.* Disruption of the sarcoglycan-sarcospan complex in vascular smooth muscle: a novel mechanism for cardiomyopathy and muscular dystrophy. *Cell* **98**, 465–474 (1999).
19. Minamisawa, S. *et al.* Chronic phospholamban-sarcoplasmic reticulum calcium ATPase interaction is the critical calcium cycling defect in dilated cardiomyopathy. *Cell* **99**, 313–322 (1999).
20. Arber, S. *et al.* MLP-deficient mice exhibit a disruption of cardiac cytoarchitectural organization, dilated cardiomyopathy, and heart failure. *Cell* **88**, 393–403 (1997).
21. Cho, M.-C. *et al.* Defective β -adrenergic receptor signaling precedes the development of dilated cardiomyopathy in transgenic mice with calsequestrin overexpression. *J. Biol. Chem* **274**, 22251–22256 (1999).
22. Rohrbach, S. *et al.* Neuregulin in cardiac hypertrophy in rats with aortic stenosis: differential expression of ErbB2 and ErbB4 receptors. *Circ.* **100**, 407–412 (1999).
23. Rochman, H.A. *et al.* Segregation of atrial-specific and inducible expression of an atrial natriuretic factor transgene in an *in vivo* murine model of cardiac hypertrophy. *Proc. Natl. Acad. Sci. USA* **88**, 8277–8281 (1991).
24. Haunstetter, A. & Izumo, S. Apoptosis: Basic mechanisms and implications for cardiovascular disease. *Circ. Res.* **82**, 1111–1129 (1998).
25. Christensen, G., Minamisawa, S., Gruber, P.J., Wang, Y.B. & Chien, K.R. High-efficiency, long-term cardiac expression of foreign genes in living mouse embryos and neonates. *Circ.* **101**, 178–184 (2000).
26. Ikeda, S., Hamada, M. & Hiwada, K. Contribution of non-cardiomyocyte apoptosis to cardiac remodeling that occurs in the transition from compensated hypertrophy to heart failure in spontaneously hypertensive rats. *Clin. Sci.* **97**, 239–246 (1999).
27. Vander Heiden, M.G. *et al.* Bcl-xL promotes the open configuration of the voltage-dependent anion channel and metabolite passage through the outer mitochondrial membrane. *J. Biol. Chem.* **276**, 19414–19419 (2001).
28. Sun, X., Liu, X.B., Martinez, J.R., Dang, H. & Zhang, G.H. Effects of radiation on Ca^{2+} signaling in salivary epithelial cell lines transfected with Bcl-2 and Bcl-XL. *Eur. J. Oral. Sci.* **109**, 103–108 (2001).
29. Young, R.C., Ozols, R.F. & Myers, C.E. The anthracycline antineoplastic drugs. *N. Engl. J. Med.* **305**, 139–153 (1981).
30. Suzuki, T. & Miyauchi, T. A novel pharmacological action of ET-1 to prevent the cytotoxicity of doxorubicin in cardiomyocytes. *Am. J. Physiol. Regul. Integr. Comp. Physiol.* **280**, R1399–R1406 (2001).
31. Lee, K.-F. *et al.* Requirement for neuregulin receptor ErbB2 in neural and cardiac development. *Nature* **378**, 394–398 (1995).
32. Erickson, S.L. *et al.* ErbB3 is required for normal cerebellar and cardiac development: a comparison with ErbB2 and heregulin-deficient mice. *Development* **124**, 4999–5011 (1997).
33. Britsch, S. *et al.* The ErbB2 and ErbB3 receptors and their ligand, neuregulin-1, are essential for development of the sympathetic nervous system. *Genes Dev.* **12**, 1825–1836 (1998).
34. Zhao, Y.-Y. *et al.* Neuregulins promote survival and growth of cardiac myocytes: Persistence of ErbB2 and ErbB4 expression in neonatal and adult ventricular myocytes. *J. Biol. Chem.* **273**, 10261–10269 (1998).
35. Agus, D., Bunn, P., Franklin, W., Garcia, M. & Ozols, R. HER-2/neu as a therapeutic target in non-small cell lung cancer, prostate cancer, and ovarian cancer. *Semin. Oncol.* **27**, 53–63 (2000).
36. Tanaka, N. *et al.* Transthoracic echocardiography in models of cardiac disease in the mouse. *Circ.* **94**, 1109–1117 (1996).
37. Chen, J. *et al.* Selective requirement of myosin light chain 2v in embryonic heart function. *J. Biol. Chem.* **273**, 1252–1256 (1998).